Journal of Alloys and Compounds 509 (2011) 10070–10074

Contents lists available at ScienceDirect

Journal of Alloys and Compounds

journal homepage: www.elsevier.com/locate/jallcom

Physical study of Sm^{3+} doped borochromate glass system

Wael Z. Tawfik[a,*], M.M. Mahdy[a], M.A.K. Elfayoumi[a], M.M. Elokr[b]

[a] Physics Department, Faculty of Science, Beni-Suef University, Beni-Suef, Egypt
[b] Physics Department, Faculty of Science, Al-Azhar University, Cairo, Egypt

ARTICLE INFO

Article history:
Received 22 May 2011
Accepted 6 August 2011
Available online 12 August 2011

Keywords:
Borate glass
Rare earth material
X-ray diffraction
IR
ESR

ABSTRACT

Sm^{3+} doped borochromate glasses of composition [xSm_2O_3–$74.5B_2O_3$–$25Li_2O$–$(0.5-x)Cr_2O_3$] with $x = 0$, 0.1, 0.2, 0.3, 0.4 and 0.5 mol% have been prepared by conventional quenching melting method. The XRD profile confirm the amorphous nature of the glass samples. The density measurements were made using Archimedes' principle of the prepared samples. Molar volume V_M, rare-earth ion concentration N and ionic radius r_p as well as field strength F have been estimated from the density measurements. The average optical basicity, Λ_{th}, electronegativity χ_{2av} and electronic polarizability α^{2-} were calculated for the prepared glass samples. Influence of rare earth ions on structural behavior in borochromate glasses have been investigated using infrared spectroscopy (IR). The structural changes have been analyzed with increasing rare earth concentration. Partial $BO_3 \leftrightarrow BO_4$ conversion as a function of rare earth concentration was observed. From the relative peak areas of BO_3 and BO_4 in structural groups the ratio N_4 has been calculated. ESR spectra were recorded at room temperature. The obtain ESR signals were used to estimate the paramagnetic susceptibility (χ).

1. Introduction

Glasses are more preferred as host matrix because of their high transparency, ease of mass production and shaping. Moreover, glasses show high dispersibility of many additives, large inhomogeneous broadening, and chemical durability as well as their unique thermal and mechanical properties [1,2]. Rare-earth ions play an important role in modern technology as active constituents of many optical materials. Their peculiar properties are due to the fact that the 4f electrons are shielded by the outer 5s and 5p bonding electrons, which lead to sharp absorption and emission lines due to weak interaction with the environment [3,4]. The rare earth elements (lanthanides) doped glasses have been a subject of interest in last decades because of their potential applications in optical devices such as solid state lasers and optical fiber communication. Although there has been a considerable number of investigations in the UV–VIS–NIR regions in order to evaluate the electronic structure and spectroscopic parameters associated with the lasing action of these lanthanide ions in crystals and solids. However, little information is known about the spectroscopic properties of such ions in glassy solids. Samarium ion can coexist in different valances in glass (+3 and +2) depending on the method of preparation. Under neutral melting condition in air, Sm^{3+} ions occur predominantly. The radiative properties of the doped ion depends on the dopant concentration as well as the chemical composition of glass and the nature of neighboring ions if more than one type of rare earth ion is present, several workers have been studied Sm spectra in various glass matrices [5–7].

In order to identify new optical devices for specific utility, or devices enhanced performance, an appropriate host has to be prepared. Borate glass are considered to be a suitable host for optical materials because of their special properties [6,8]. But its applications are restricted due to its high phonon energy. Borate glasses in particular, have been the subject of numerous infrared studies in order to study their structure peculiarities [9,10]. The IR spectroscopy is the most advantageous tool for the study of structural features of amorphous materials. The vibration modes of borate network are seen to be mainly active in three different spectral regions (1200–1600), (800–1200) and around 700 cm^{-1} which are similar to those reported by several workers [11,12].

Transition metal ions are being greatly used in the present days to probe the glass structure since their outer d-electron orbital functions have a broad radial distribution and due to their high sensitive response to the changes in the surrounding actions. Among various transition metal ions, the chromium ion, a paramagnetic metal ion, when dissolved in glass matrices in very small quantities makes the glasses colored and has a strong influence over the optical transmission and the insulating strength of the glasses, since it exists in different oxidation states viz., Cr^{3+}-(acting as modifier with CrO_6 structural units) and Cr^{6+}-(acting as network former with CrO_4^{2-} structural units). The content of chromium in different states with different structural units in the glass depends on

* Corresponding author. Tel.: +20 12 1764 428.
E-mail address: drwael_7@yahoo.ca (W.Z. Tawfik).

0925-8388/$ – see front matter © 2011 Elsevier B.V. All rights reserved.
doi:10.1016/j.jallcom.2011.08.037

the quantitative properties of modifiers and glass formers, size of the ions in the glass structure, their field strengths, mobility of the modifier cation, etc. Further, the most common optical absorption transition, $^4A_2 \rightarrow {}^4T_2$ (which has a strong bearing on the luminescence efficiency) of Cr^{3+} ion is found to be very sensitive to its chemical environment. Extensive investigations on the optical absorption, luminescence and ESR spectroscopy of Cr ion in a variety of inorganic glasses have been made in the recent years in view of their importance in the development of tunable solid state lasers and new luminescence materials [13–17].

In the present work the physical properties of Sm^{3+} doped borochromate glasses were investigated. IR spectra in the range of (400–4000 cm^{-1}) have been recorded and analyzed. The influence of the Cr_2O_3 content on the local symmetry and spectroscopic feature has been investigated.

2. Procedure

The method of glass preparation is the same as that described in our earlier paper [18]. The composition of the glasses studied in the present work are xSm_2O_3–$74.5B_2O_3$–$25Li_2O$–$(0.5-x)$ Cr_2O_3 with x = 0, 0.1, 0.2, 0.3, 0.4 and 0.5 mol%. The prepared glasses had good transparency and were circular in shape with a uniform thickness of about 0.2 cm. The glass samples of uniformly transparent were chosen for optical studies. The powder samples were prepared by crushing and grinding the glass pieces in an agate mortar. The powder was used for measurements of IR and ESR spectroscopy. The glass system was examined by X-ray diffraction (XRD) at room temperature. The density of the prepared glass system was determined at room temperature by simple Archimedes' principle using toluene as immersion liquid (ρ_0 = 0.886 g/cm^3). The molar volume was calculated by using the measured density and molecular weight of glass. Infrared spectra were measured at room temperature using FT-IR PerkinElmer in the range of 400–4000 cm^{-1}. The ESR spectra were recorded at room temperature using ESR spectrometer (EMX-Bruker)-operating in X-band frequency.

3. Results and discussion

XRD patterns of the glass sample are shown in Fig. 1; no diffraction peaks were observed which confirm the amorphous nature of the glass samples. The measured and calculated values of the density (ρ) along with the molar volume (V_M) are listed in Table 1 and shown in Fig. 2. The density increases linearly from 2.147 to 2.299 (g/cm^3) as Sm_2O_3 content increases from 0 to 0.5 mol%. The increase in density can be accounted for by the difference in the atomic mass and atomic radii of Cr and Sm, where the atomic mass of Cr and Sm atoms are 51.9961 and 150.36, respectively and their atomic radii are 1.66 Å and 2.38 Å, respectively. The difference in ionic radii leads to higher compactness by Sm addition. In this respect Sm ions exhibit large coordination number [19]. The observed compactness also may be related to the transformation of BO_4 to BO_3 structural

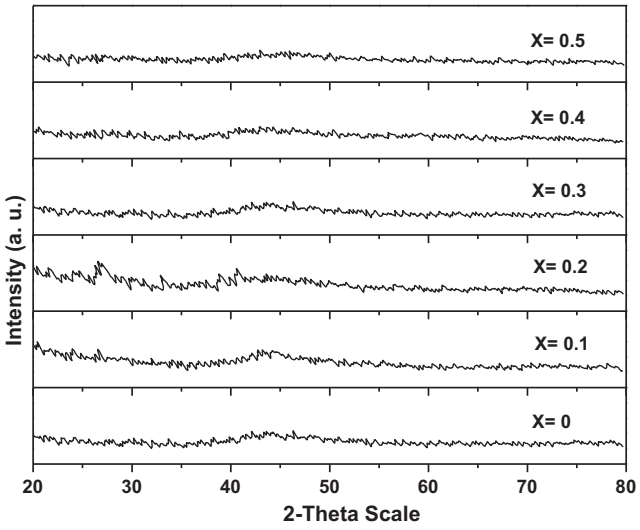

Fig. 1. X-ray pattern for the glass system.

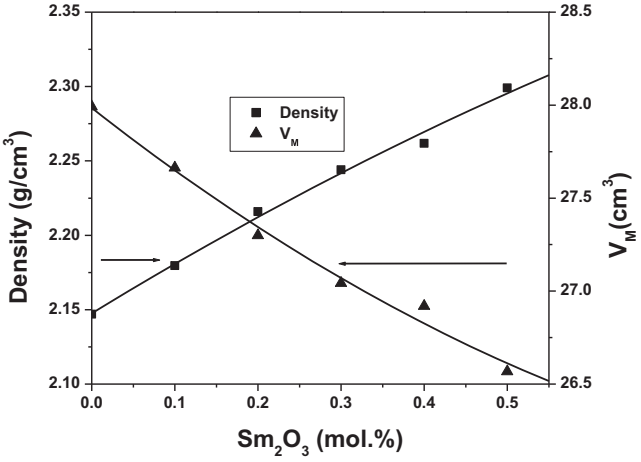

Fig. 2. Density and molar volume as a function in Sm_2O_3 content.

units [20]. The behavior of molar volume follows a trend opposite to that of density which is the normal expected behavior. The rare earth ion concentration (N) is calculated using the formula [21]:

$$N(\text{ions/cm}^3) = \frac{[N_A(\text{mol\% of rare earth})\rho]}{M}$$

where N_A is the Avogadro's number, ρ is the density and M is the average molecular weight. The obtained values of N are listed in Table 1. It is observed that the concentration N increases with increasing of Sm_2O_3 content as shown in Fig. 3. It should be mentioned that the samarium ions are assumed to be uniformly

Table 1
Physical properties of the prepared glass samples.

X mol%	0	0.1	0.2	0.3	0.4	0.5
$\rho_{exp.}$ (g/cm^3)	2.146908	2.179608	2.215853	2.244082	2.26174	2.299055
$\rho_{th.}$ (g/cm^3)	2.153612	2.207324	2.260004	2.311683	2.362388	2.412147
V_m (cm^3)	27.99253	27.66282	27.29911	27.04335	26.91923	26.56783
$N \times 10^{20}$ (ion/cm^3)	–	0.218	0.441	0.668	0.895	1.13
$r_p \times 10^{-7}$ (Å)	–	1.44	1.14	0.993	0.901	0.833
$F \times 10^{15}$ (cm^{-2})	–	2.98	4.77	6.29	7.64	8.94
X_{2av}	2.609240	2.609044	2.608848	2.608652	2.608456	2.608260
Λ_{th}	0.59559	0.59569	0.59578	0.59588	0.59597	0.59606
$\alpha^{2-} \times 10^{-24}$ (cm^3)	1.55608	1.55621	1.55635	1.55648	1.55662	1.55675
N_4	0.242002	0.253154	0.340874	0.362265	0.351731	0.36605

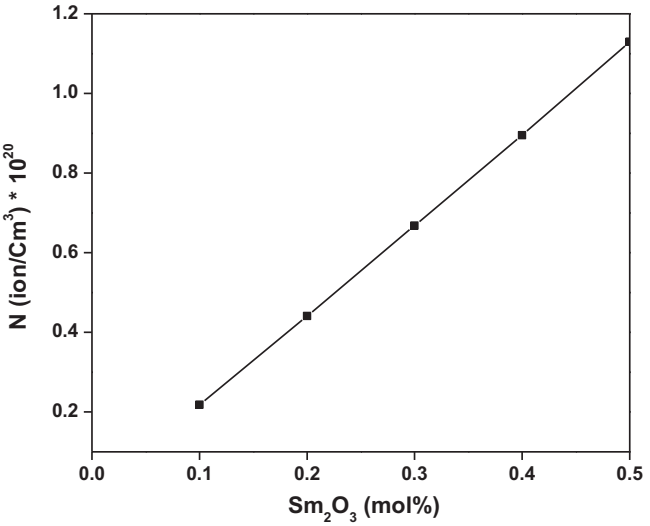

Fig. 3. The relation between the rare earth ion concentration (N) and Sm_2O_3 content.

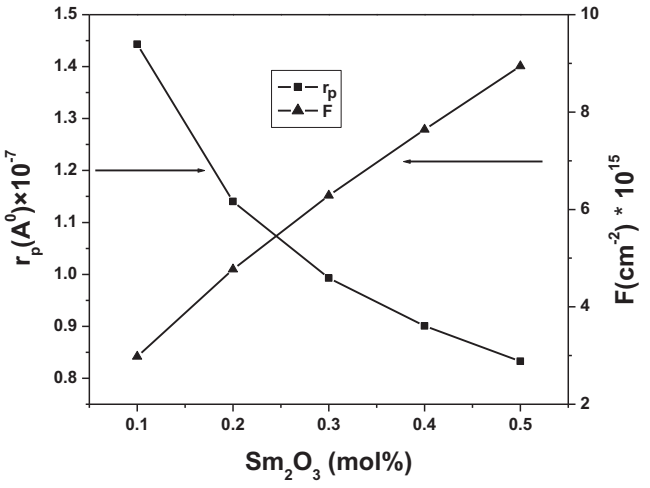

Fig. 4. Field strength (F) and ionic radius (r_p) as a function of Sm_2O_3 content.

distributed in the glass matrix [19]. The obtained values of N are used to calculate the ionic radius (r_p) according to the relation [22]:

$$r_p(A^0) = \frac{1}{2}\left[\frac{\pi}{6N}\right]^{1/3}$$

The estimated values of r_p are presented in Table 1 and are shown in Fig. 4. From the figure, it is clear that the estimated values of r_p decreases by the increases of Sm_2O_3 content in the glass composition [23]. This may be attributed to the enhanced compactness observed with Sm_2O_3 addition. It is worth mentioning that the rare earth ions are situated between the layers and thus the average rare earth-oxygen distance decreases. As a result of that, the Sm–O bond strength increases, producing stronger field strength (F) around Sm^{3+} ions as shown in Fig. 4 [19]. The field strength around Sm^{3+} ion is calculated according to the equation [23]:

$$F = \frac{Z}{r_p^2}$$

where Z is the atomic mass of the Sm ion and r_p is the ionic radius. The obtained values F are listed in Table 1.

The average optical basicity serves in the first approximation as a measurement of the ability of oxygen to donate negative charge

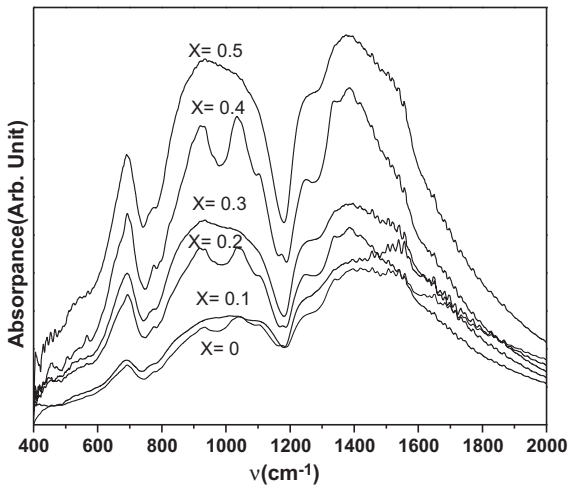

Fig. 5. The IR spectra for the prepared glass samples.

in the glass samples [21]. The average optical basicity, Λ_{th}, for the glass system under study was estimated using the electronnegativity (χ_{2av}) for the oxides used in the glass system through the formula:

$$\Lambda_{th} = \frac{0.75}{\chi_{2av} - 1.35}$$

The average electronic polarizability α^{2-} was estimated according to the relation [24]:

$$\alpha_0^{2-} = \frac{\chi_{2av} - 1.35}{\chi_{2av} - 1.80}$$

The calculated values of Λ_{th}, χ_{2av} and α^{2-} are included in Table 1. It is clear that the value of Λ_{th} increases with the increase in mol% of Sm_2O_3, i.e. the degree of covalency of the glass is decreased. It is most likely to assume that the increasing Λ_{th} with increasing of Sm content means increasing the polarizability values and hence the increase of the bond strength. This can explain the observed increase of density by increasing Sm content.

The IR spectra at the room temperature over the range of 400–4000 cm^{-1} for the prepared glass samples are shown in Fig. 5. The boron ion is a glass network forming cation and it may occupy the centers of oxygen triangles or tetrahedral [25]. In order to get qualitative information about the structural groups in the samples, the experimental observed bands were subjected to deconvolution (assuming Gaussian line form), Fig. 6 illustrated the results of the deconvolution for (0.5 mol% Sm sample). The IR spectra show eight absorption peaks the peaks are sharp, medium, and broad. The broad bands are exhibited in the oxide spectra, most probably due to the combination of high degeneracy vibrational states, thermal broadening of the lattice dispersion band and mechanical scattering from powder samples [25]. In the present work the mid-IR region consists of many bands around (690, 920, 1040, 1180, 1350, 1500 cm^{-1}) connected with less intense bands or shoulder in the ascending or descending lobes of these sharp bands at about (820, 1250 cm^{-1}). In the samples containing chromium, it is obvious that the chromium ions have only minor effect on the IR spectra of the studied glasses this may be due to the low content of chromium (maximum chromium value = 0.5 mol%), so the structural groups remain unchanged giving their characteristic vibration. From the relative peak areas of BO_3 and BO_4 in structural groups, which separated by Gaussian deconvolution, the ratio N_4 was calculated using the relation [26]:

$$N_4 = \frac{BO_4}{BO_4 + BO_3}$$

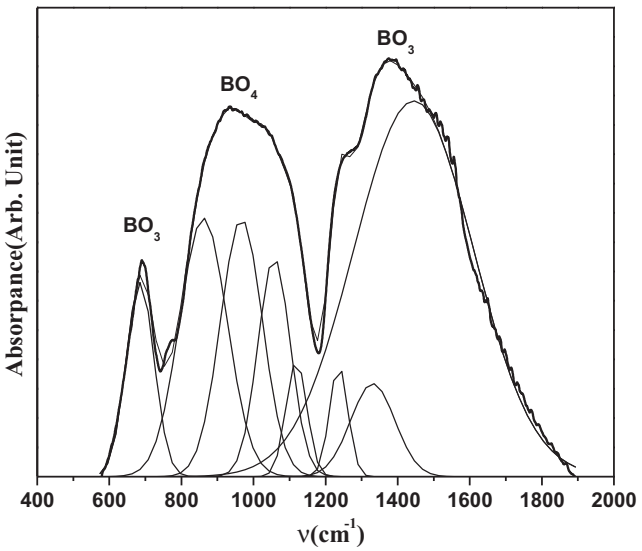

Fig. 6. The IR spectrum for $x = 0.5$ is deconvoluted.

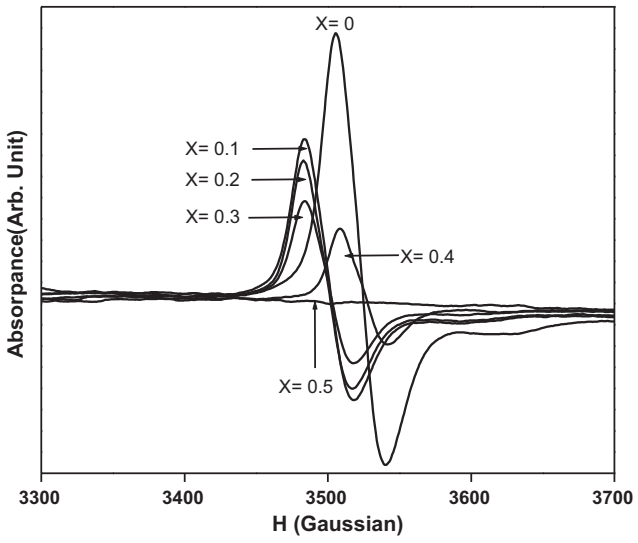

Fig. 8. ESR signal of prepared glass samples.

where BO_4 is the area of BO_4 units, calculated in the range (800–1200 cm^{-1}), and BO_3 is the area of BO_3 units, calculated in the range (1200–1600 cm^{-1}). The dependence of the ratio N_4 on samarium content is shown in Fig. 7 and listed in Table 1. It is observed that, the values of N_4 are less than unity, showing the predominance of BO_3 units in these glass structure this can be accounted for by the low content of network modifier (max. value 25% Li_2O). It is clear that, the ratio N_4 increases by increasing Sm_2O_3 concentration revealing the transformation of BO_3 to BO_4 units. This is in good agreement with the density measurements (i.e. structure become more compact); also similar behavior was observed in europium doped borate glass [27].

ESR of chromium ions in glasses is very interesting because its valence state may change with the variation of glass composition and preparation conditions. Fig. 8 reveals ESR signals of the investigated samples. It is clear that, all samples exhibit ESR signal except the chromium-free sample ($x = 0.5$). This indicates that the host glass is free from any paramagnetic centers, which means that the observed signals are only due to Cr^{3+} ions (d^3 configuration). As the concentration of chromium ion increased gradually up to 0.5 mol% two signals, one at $g = 1.98$ and the other at $g \sim 5$ should be observed [28–30]. However, in the present study only one signal has been observed, which is due to the available range of the magnetic fields. The observed behavior suggested that the Cr ions are of trivalent state and acted up on by octahedral ligand field. In an octahedral field, the ground level of the Cr^{3+} (d^3) ion is $^4A_{2g}$; under the action of a low symmetric field component and spin orbit coupling, the fourfold degenerate spin state splits into two Kramers doublets $\pm 3/2\rangle$ and $\pm 5/2\rangle$ [31,32]. The separation between these two doublets leads to the resonance at $g = 2$ to $g \sim 5$. According to the theory of Landry, the low field line with $g \sim 5$ is attributed to the isolated Cr^{3+} ions that have local rhombic sites subjected to strong crystal field effects. This signal arises mainly due to $-3/2 \leftrightarrow +3/2$ that are allowed due to low symmetry of Cr^{3+} ions. Comparatively larger intensity of low field peak ($g \sim 5$) indicates higher concentration of isolated Cr^{3+} ions in this glass network [31]. In the present work the resonance signal at $g \sim 5$ was not be observed because it is out of range of the spectrometer (low external field). The intensity and the line width of the resonance signal at $g \sim 1.98$, arises due to the exchange coupling between Cr^{3+} and Cr^{3+} ion pairs, are observed to increase with increase in the concentration of chromium ions. Such an increase indicates the increase of chromium ions in Cr^{3+} state in the glass network and also the near absence of antiferromagnetic interactions between Cr^{3+} ions [31]. This can be confirmed from Fig. 9, in which the number of spins participating in resonance (spin density N) increase with the increase of Cr-content. The obtained spectra were analyzed using axial Spin-Hamiltonanian [33]. The ESR parameters $g_\parallel$, $g_\perp$, $A_\parallel$, and $A_\perp$ are calculated and listed in Table 2. In the present work the spin of chromium nucleus is zero ($I = 0$) gives no orientation, i.e. no coupling constant was found ($A_\parallel$, and $A_\perp = 0$) as shown from Fig. 8. The value of $\Delta g_\parallel / \Delta g_\perp$, where $\Delta g_\parallel = (g_e - g_\parallel)$ and $\Delta g_\perp = (g_e - g_\perp)$ measures the tetragonal distortion around the ions [34]. The values of $\Delta g_\parallel / \Delta g_\perp$ tend to increase with concentration of Cr-ions (decrease with Sm-content) as shown in Fig. 10. This implies that as the concentration increase, the deviation from the ideal octahedral symmetry increase and the CrO_4^{2-} ions become more tetragonally distorted. The obtained ESR parameters were used to calculate the paramagnetic susceptibility of the sample using the formula:

$$\chi = \frac{Ng^2\beta^2 j(j+1)}{3k_B T}$$

where N is the number of spins per m^3 (spin density), the rest of the symbols have their usual meaning, $g = (g_\parallel + 2g_\perp)/3$. The values of χ

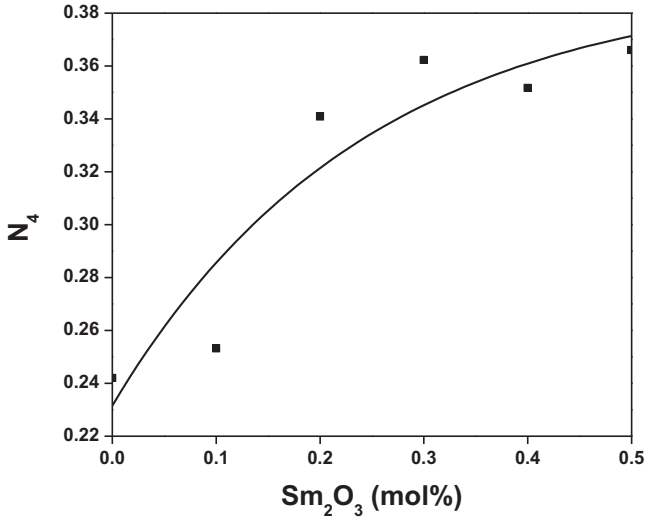

Fig. 7. The relation between N_4 and the Sm_2O_3 content.

Table 2
The values of ESR parameters.

X mol%	$g_{\parallel}$	$g_{\perp}$		$A_{\parallel}$	$A_{\perp}$	$\Delta g_{11}/\Delta g_{\perp}$	$N \times 10^{18}$	$X \times 10^{-9}$	$1/X \times 10^{8}$
0	1.98	–		–	–	0.011137	5.07	11.4	0.87
0.1	1.9802	–		–	–	0.011037	3.8	8.59	1.16
0.2	1.98037	–		–	–	0.010952	3.27	7.39	1.35
0.3	1.98073	–		–	–	0.010773	2.51	5.68	1.76
0.4	1.98168	–		–	–	0.010244	1.14	2.58	3.78

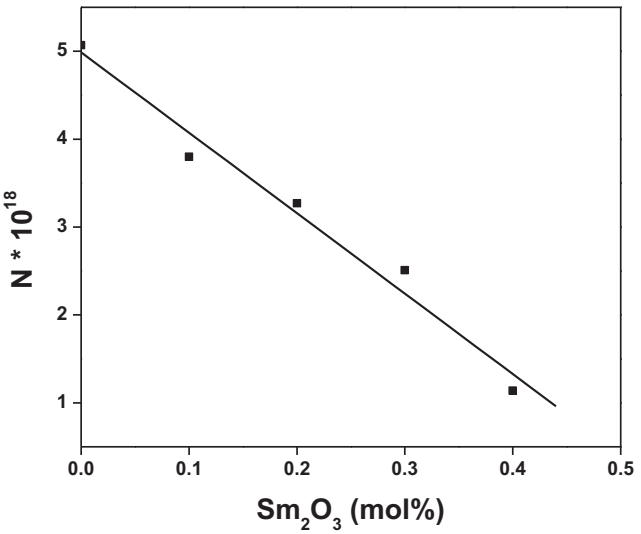

Fig. 9. The relation between number of spin density (N) and Sm_2O_3 content.

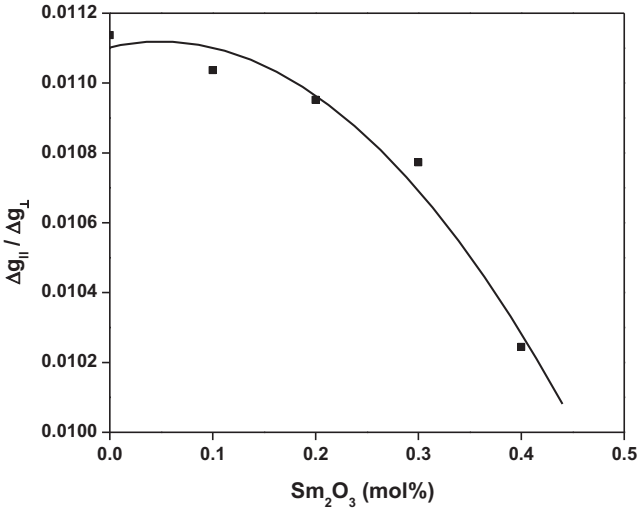

Fig. 10. The relation between the ratios ($\Delta g_{\parallel}/\Delta g_{\perp}$) and Sm_2O_3 content.

as well as the reciprocal of paramagnetic susceptibility ($1/\chi$) were listed in Table 2. It is clear that, it follow the same trend as spin density. Inspection of the table reveals that g-value is slightly less than that of free electron ($g_e = 2.0036$) indicating that the electron is slightly more free in a particular orbital about the atom.

4. Conclusions

Glassy system of composition:

$$x Sm_2O_3 – 74.5B_2O_3 – 25Li_2O – (0.5 - x)Cr_2O_3$$

where $x = 0$, 0.1, 0.2, 0.3, 0.4 and 0.5 mol% has been prepared by a conventional quenching melting technique. It is observed that the XRD data confirm the amorphous nature of the prepared glass samples. The density increases by increasing Sm-content while as the molar volume follows the opposite trend. On the other hand the field strength increases by increasing Sm-content. The optical basicity and polarizability are almost independent of the composition. IR spectra indicate that both Sm_2O_3 and Cr_2O_3 have minor effect on the boron structural units. However, the ratio N_4 was found to increase with Sm_2O_3 content revealing the transformation of $BO_3 \leftrightarrow BO_4$. No ESR signals are observed for Cr-free sample indicating the absence of paramagnetic centers and reveals that the observed ESR signal is only due to Cr^{3+} ions.

References

[1] K. Arun Varshneya, Fundamental of Inorganic Glasses, Academic Press, San Diego, 1994.
[2] Bach. Neuroth, The Properties of Optical Glass, Springer-Berlin, 1995.
[3] G. Liu, B. Jacquier, Spectroscopic properties of rare earths in optical materials, Springer series in mater. sci., 2005.
[4] C.W. Thiel, PhD, Montana State University, 2003.
[5] H. Lin, E.Y.B. Pun, X. Wang, X. Liu, J. Alloys Compd. 390 (2005) 197.
[6] H. Lin, D. Yang, G. Liu, T. Ma, B. Zahi, Q. An, J. Yu, X. Wang, X. Liu, E.Y.B. Pun, J. Lumin. 113 (2005) 121.
[7] G. Tripathi, V.K. Rai, Opt. Commun. 264 (2006) 116.
[8] N. Soga, K. Hirao, M. Yoshimoto, H. Yamamoto, J. Appl. Phys. 63 (1988) 4451.
[9] E.L. Kamitsos, M.A. Karakassides, J. Phys. Chem. Glasses 30 (1989) 19.
[10] L. An, J. Zhang, M. Liu, S. Chen, S. Wang, Opt. Mater. 30 (2008) 957.
[11] E.L. Kamitsos, M.A. Karakassides, G.D. Chryssikos, J. Phys. Chem. Glasses 91 (1987) 1073.
[12] F.M. Ezz Eldin, N.A.E.L. Alaily, F.R.A. Khalifa, H.A.E.L. Batal, Third ESG Conference, 1995.
[13] T.R.N. Kutty, Mater. Res. Bull. 25 (1990) 485.
[14] G. Srinivasarao, N. Veeraiah, EPJ. Appl. Phys. 16 (2001) 12.
[15] J.L. Rao, B. Sreedhar, M.R. Reddy, S.V. Lakshman, J. Non-Cryst. Solids 111 (1989) 228.
[16] A. Van Die, A.C.H.I. Leenaers, W.F. Van Der Weg, J. Non-Cryst. Solids 99 (1988) 32.
[17] M. Rami Reddy, V. Ravi Kumar, N. Veeraiah, Ind. J. Pure Appl. Phys. 33 (1995) 48.
[18] Y.C. Ratnakaram, R.P.S. Chakradhar, K.P. Ramesh, J.L. Rao, J. Ramakrishna, J. Mater. Sci. 38 (2003) 833.
[19] A. Mekki, K.A. Ziq, Holland, J. Magn. Magn. Mater. 260 (2003) 60.
[20] W.A. Pisarski, J. Ppisarska, W. Ryba-Romanowski, J. Mol. Struct. 744–747 (2005) 515.
[21] A. Murali, J. Lakshmana Rao, A. Venkata Subbaiah, J. Alloys Compd. 257 (1997) 96.
[22] Y.C. Ratnakaram, D. Thirupathi Naidu, A. Vijaya Kumar, N.O. Gopal, Physica B 358 (2005) 296.
[23] S. Mandal, A. Ghosh, Phys. Rev. B 48 (1993) 9388.
[24] J.A. Duffy, J. Non-Cryst. Solids 297 (2002) 275.
[25] S.G. Motke, S.P. Yawale, S.S. Yawale, Bull. Mater. Sci. 25 (2002) 75.
[26] R.C. Lucacel, C. Marcus, V. Timar, I. Ardelean, Solid State Sci. 9 (2007) 850.
[27] E. Culea, T. Ristoiu, I. Bratu, D. Ristoiu, Mater. Sci. Eng. B 75 (2000) 82.
[28] I. Ardelean, Gh. Ilonca, M. Peteanu, E. Barbos, J. Mater. Sci. 17 (1982) 1988.
[29] C. Laxmi Kanth, N. Veeraiah, J. Quant. Spectrosc. Radiative Transf. 90 (2004) 97.
[30] M. Haouari, H. Ben Ouada, H. Maaref, H. Hommel, P. Legrand, Phosphors Res. Bull. 6 (1997) 241.
[31] G. Little Flower, M. Srinivasa Reddy, G. Sahaya Baskaran, N. Veeraiah, Opt. Mater. 30 (2007) 357.
[32] G. Murali Krishna, B. Anila Kumari, M. Srinivasa Reddy, N. Veeraiah, J. Solid State Chem. 180 (2007) 2747.
[33] O. Cozar, I. Ardelean, I. Bratu, S. Simon, C. Cracium, L. David, C. Cefan, J. Mol. Struct. 563–564 (2001) 421.
[34] R.P. Sreekanth Chakradhar, A. Murali, J. Lakshmana Rao, Physica B 293 (2000) 108.